China Geology 8 (2025) 253−264

China Geology

Journal homepage: http://chinageology.cgs.cn
https://www.sciencedirect.com/journal/china-geology

Synergistic effects of potassium-silicon-calcium mineral fertilizer combined with rice husk biochar on the immobilization of Cd and Pb in soil

Cheng-jie Zou[a], Ze-ming Shi[a, b,*], Na Zhang[a], Ying-hai Zhu[a], Lü-han Yang[c], Xin-yu Wang[a]

[a] *College of Earth and Planetary Sciences, Chengdu University of Technology, Chengdu* 610059, *China*
[b] *Sichuan Province Key Laboratory of Nuclear Techniques in Geosciences, Chengdu* 610059, *China*
[c] *Sichuan Tianshengyuan Environmental Services Co., Ltd, Chengdu* 610037, *China*

ARTICLE INFO

Article history:
Received 31 May 2023
Received in revised form 15 November 2023
Accepted 3 September 2024
Available online 12 October 2024

Keywords:
Heavy metal
Cadmium
Lead
Mineral fertilisers
Biochar
Adsorption experiment
Equilibrium adsorption
Soil column leaching experiment
Agricultural geological survey engineering

ABSTRACT

The combined application of mineral fertilizer and biochar significantly improves the passivation of heavy metal-contaminated soil, surpassing the effects of individual application. This study has reinforced the validation of their passivation competence as soil remediation agents by examining the multifaceted role of potassium-silicon-calcium mineral fertilizer combined with rice husk-based biochar generated at different pyrolysis temperatures. The soil leaching column experiment, conducted based on the adsorption experiments, has facilitated our scrutiny of the passivation impacts of cadmium (Cd) and lead (Pb) when introducing different proportions of mineral fertilizers and biochar into the soil. These results indicate that biochar's adsorption efficiency for Cd and Pb is significantly improved at escalated pyrolytic temperature conditions in a single solution. The biochar generated at 700°C (C700) renders adsorption effectiveness of approximately 84.24% for Cd and 99.74% for Pb. Biochar conspicuously registers superior adsorption efficiency towards Pb relative to Cd. The mineral fertilizer, which achieves an adsorption efficiency of 97.76% for Cd, is identified as the main adsorbent for Cd, although its competence is slightly lower compared to C700 for Pb adsorption. Within a complex solution, biochar and mineral fertilizer show reduced Cd and Pb adsorption levels compared to single solutions. There is a keen competition for adsorption surfaces witnessed between Cd and Pb, with Pb's distribution coefficient (K_d) notably outpacing that of Cd. The isothermal adsorption analyses depict that the mineral fertilizer follows the Langmuir model for Cd adsorption, while C700 conveys the Freundlich model for Pb adsorption. The soil leaching column experiment's results signify that the composite passivation agents significantly outperform the individual passivation agents in efficiency. The combined application of biochar and mineral fertilizer minimizes the cumulative leaching of Cd and Pb, with the optimal soil remedy proportion for heavy metal contamination being 7∶3. In practical application, mindful consideration should be accorded to the deployment ratios of different passivation agents.

1. Introduction

Soil contamination hampers sustainable agricultural progression and can potentially cause issues concerning the ecosystem, public health, and societal developments (Yang L et al., 2018; Liu RP et al., 2020). Anthropogenic activities have generated hazardous heavy metals, such as Cd and Pb, which pose significant health risks due to their high migration and accumulation ability in the soil (Bao LR et al., 2020; Xu HL et al., 2021). The prolonged accumulation of high concentrations of heavy metals can result in decreased oxygenation, porosity, and microbial activity in the soil, which hampers plant root development and the adsorption and transfer of beneficial elements. Furthermore, these heavy metals can permeate the human body through skin contact, inhalation, and indirectly via the food chain, posing a significant threat to human health (Wang P et al., 2019; Lin J et al., 2021). Consequently, the urgent development of an environmentally friendly soil heavy metal remediation agent has become imperative to alleviate and manage soil heavy metal contamination.

The use of passivation agents in soil treatment is critical in

First author: *E-mail address*: sdchex@gmail.com (Cheng-jie Zou).

* Corresponding author: *E-mail address*: shizm@cdut.edu.cn (Ze-ming Shi).

Literary editor: Xi-jie Chen
doi:10.31035/cg20230050
2096-5192/© 2025 China Geology Editorial Office.

responding to heavy metal pollution. This approach employs the unique physicochemical attributes of passivation agents to capture and modify the valence and availability states of heavy metals, significantly curbing their mobility and toxicity. Biochar, a restorative material of natural abundance, is characterized by a vast specific surface area, excellent pore structure, and cost-effectiveness, originating from a wide range of sources. Its potential in restoring metal-contaminated soils has demonstrated significant promise (Liang LP et al., 2021; Rushimisha IE et al., 2022; Zhang K et al., 2023). Generated through the pyrolysis of agricultural by-products under temperatures below 700°C thermal conditions in an optimally oxygen-limited setting, this carbon-dense substance has been effectively harnessed in environmental restoration efforts, particularly owing to its highly effective in reducing the mobility of heavy metals in soil (Yin D et al., 2017). Notwithstanding, the pyrolytic generation of biochar is marred by its high volatility and a glaring lack of encapsulation, resulting in heavy carbon losses and consequentially compromising its adsorptive capacity. Moreover , the nutritional content in common variants of biochar falls short of the requisite levels. Therefore, one can noticeably elevate biochar's efficiency by modifying the original substance or pairing it with other passivation agents. An example is mineral fertilizer, synthesized by mimicking the natural rocky weathering using hydrothermal methods. This substance improves heavy metal-contaminated soil and releases elements such as potassium and silicon during continued weathering, thereby elevating soil fertility. Due to their large specific surface area and porous structure, weathered silicate minerals can adsorb and immobilize most heavy metals, thereby reducing their incidence in crops and enhancing crop quality (He YB et al., 2017; Xu Y et al., 2017). Integrating biochar with a mineral fertilizer as a passivation agent presents a mutually beneficial proposition, amplifying the stability of the passivation, refining the soil texture, and shielding crops against metals elements (Osman AI et al., 2022)

Primarily, the use of modified biochar or their combinations with iron compounds, alkali slag, limestone and numerous other materials constitutes the mainstream applications of biochar in the passivation of heavy metal adsorption. However, despite our country's escalating promotion of mineral fertilizers, concentrating particularly on their effects on plant growth, research remains scant in combining mineral fertilizers and biochar for Cd and Pb adsorption and soil leaching attributes. Consequently, this study examines Cd and Pb adsorption characteristics and soil remediation impacts of rice husk biochar, mineral fertilizer, and different combinations of mineral fertilizer and biochar through adsorption and leaching experiments. Furthermore, this study aims to identify the optimal proportion of combined usage of mineral fertilizer and biochar, hoping to provide theoretical and technical support for the application mineral fertilizers in Cd and Pb contaminated soils.

2. Materials and methods

2.1. Materials

The mineral fertilizers used in the experiment were sourced from Sino-Mineral Technology. The basic components of these fertilizers are CaO (35.8%), SiO_2 (20.3%), K_2O (5.7%), Fe_2O_3 (5.1%), and MgO (1.1%). After being desiccated at a temperature 40°C in drying ovens, the mineral fertilizers are pulverized into fine particles. Subsequently, they are screened through an 80-mesh sieve. The resulting ground product is then reserved for future application and labelled "M".

The rice husks used in biochar production, harvested from Mianyuan Town, Shifang City, were thoroughly cleaned of impurities, such as leaves and grass, using an ultrasonic cleaner with deionized water. After being dried at a temperature of 40°C in a drying oven, five portions of dried rice husks were individually subjected to pyrolysis at 300°C, 400°C, 500°C, 600°C, and 700°C for 120 minutes in a muffle furnace. After cooling to ordinary temperature, the resulting specimens were extracted and finely ground through a 200-mesh sieve to obtain high-quality rice husk biochar. These biochar samples were labelled as C300, C400, C500, C600, and C700, respectively, and were stored in sealed containers for future use. The characteristics of biochar (700°C) and mineral fertilisers are shown in Table 1.

2.2. Characteristics of soil and passivation agents

The soil samples employed in the experiment were gathered from Shigu Town, Shifang City, situated in the Sichuan Province (104°05′17.48″ E, 31°05′46.40″ N). Upon removing the uppermost layer of soil, the surface soil with a depth ranging from 5−20 cm was extracted using a bamboo shovel and carefully deposited into polypropylene bags. Subsequently, the samples underwent natural air-drying at ordinary temperature, purification, moderate grinding, and sieving through a 10-mesh screen. Finally, the samples were transferred into clean sample bags to prepare for the subsequent experiments. The characteristics of soil is shown in Table 1.

The soil utilised in the experiment is slightly acidic, with Cd and Pb concentrations of 4.11 μg/g and 39.7 μg/g, respectively. The Cd content surpasses the regulated threshold for soil contamination risk in agricultural land, which is 2.0 μg/g (5.5<pH⩽6.5). Conversely, the Pb content is below the established threshold for soil contamination risk in

Table 1. Characteristics of soil and passivation agents.

Samples	BET surface area (m^2/g)	pore volume (cm^3/g)	pore size(nm)	pH	Pb(μg/g)	Cd (μg/g)
Soil	–	–	–	5.94	39.7	4.11
Biochar (700°C)	234.61	0.16	2.70	9.68	2.91	0.26
Mineral fertilisers	40.06	0.057	6.18	10.98	10.96	0.32

agricultural land, which is 90 μg/g (5.5<pH⩽6.5) as specified by GB 15618-2018. The mineral fertiliser and rice husk biochar are alkaline and exhibit lower content of Cd and Pb compared to the soil. Consequently, incorporating mineral fertilizer and rice husk biochar into the soil for remediation will not result in secondary pollution.

2.3. Research methodology

2.3.1. Adsorption experiment

Conduct single-solution and complex-solution adsorption experiments to determine the adsorption characteristics of biochar and mineral fertilisers on heavy metals. In the single-element adsorption experiment, two groups of 0.1 g passivation agents (C300, C400, C500, C600, C700, M) were placed in 50 mL test tubes. To the first group, add 25 mL of Cd^{2+} solution with a concentration of 20 mg/L (pH=5.5), and to the second group, add 25 mL of Pb^{2+} solution with a concentration of 60 mg/L (pH=5.5). Shake the tubes at a constant temperature of 25°C and a shaking speed of 190 r/min for 24 hours. After completion, centrifuge the tubes at a rate of 4000 r/min for 10 min, take 10 mL of the supernatant, and filter it through a 0.45 μm membrane. Then, measure the content of Cd and Pb in the solution. Repeat each experiment three times.

In the experiment involving the adsorption of a complex solution, the solution was formulated based on the Pb-to-Cd ratio found in the surface soil of Sichuan Province (Shi ZM, 2014). The concentrations of Pb and Cd were set at 60 mg/L and 20 mg/L, respectively, with a concentration ratio of 3:1, and a pH of 5.5 was maintained. A weight of 0.1g of the passivation agents (C300, C400, C500, C600, C700, M) was accurately measured and placed into a 50 mL test tube. Subsequently, 25 mL of the Cd-Pb mixed solution was added. The remaining steps followed the protocol of the single-solution adsorption experiment.

In the adsorption experiment of the complex solution with composite inhibitors, 0.05g of the C700 and M passivation agents were individually weighed and placed into 50 mL test tubes. Then, 25 mL of the Cd and Pb complex solution was added. The remaining steps were consistent with the single solution adsorption experiment, including three replicate samples for each condition.

Formulas for determining the removal efficiency (r, %) and adsorption capacity at time t (q_t, mg/g):

$$q_t = \frac{(C_0 - C_t) \times V}{m} \tag{1}$$

$$r = \left(\frac{C_0 - C_e}{C_0} \right) \times 100\% \tag{2}$$

In the equation, C_0, C_t, and C_e represent the initial, time t, and equilibrium concentrations of Cd^{2+} and Pb^{2+} in the solution, measured in mg/L. V denotes the volume of the Cd^{2+} solution added, measured in mL, and m is the total mass of the adsorbent material added, measured in g.

2.3.2. Isothermal adsorption experiment

In the isothermal adsorption experiment, the concentrations of the Cd and Pb solutions varied within specific ranges. The Cd solution had concentrations of 5 mg/L, 10 mg/L, 20 mg/L, 40 mg/L, 80 mg/L, 120 mg/L, 160 mg/L, 240 mg/L, and 320 mg/L, while the Pb solution had concentrations of 15 mg/L, 30 mg/L, 60 mg/L, 80 mg/L, 100 mg/L, 120 mg/L, 160 mg/L, 240 mg/L, and 320 mg/L. The pH of the solution remained constant at 5.5. A weight of 0.1 g of passivation agents and a solution volume of 25 mL were used for the adsorption process. All other steps in the experiment were kept consistent with the adsorption procedure. The experimental data were analysed by fitting it to the Langmuir and Freundlich models, with the expressions shown below:

$$\text{Langmuir}: q_e = \frac{q_m K_L C_e}{1 + K_L C_e} \tag{3}$$

$$\text{Freundlich}: q_e = K_F C_e^{1/n} \tag{4}$$

In the equation, q_e denotes the amount of Cd or Pb adsorbed at equilibrium, C_e (mg/g) represents the concentration of Cd^{2+} or Pb^{2+} at equilibrium adsorption, q_m (mg/g) represents the maximum adsorption capacity estimated by the Langmuir model. K_L (L/mg) signifies the rate of the adsorption to the desorption. K_F ($L^{1/n} \cdot mg^{1-1/n} \cdot g^{-1}$) is the constant of the Freundlich model, where $1/n$ signifies the adsorption intensity or surface heterogeneity.

2.3.3. Soil leaching column experiment

Through conducting leaching experiments to simulate the variations in the leaching of Pb and Cd under natural precipitation conditions, this study assesses the fixation efficiency of different passivation on Cd and Pb in the soil while also investigating the optimal proportion of mineral fertiliser and biochar. The annual precipitation in the experimental area ranges from 794–817 mm, with rainfall typically being acidic. The principal influent ions encompass SO_4^{2-}, Ca^{2+}, Mg^{2+}, NO_3^-, and NH_4^+ (Zhang JJ, 2021; Lv XY et al., 2022). Before the experiment, anhydrous $CaCl_2$, $MgSO_4 \cdot 7H_2O$, $MgCl_2 \cdot 6H_2O$, and HNO_3 were applied to adjust the ion concentration of the leachate, accurately mimicking natural rainfall conditions, and HCl was used to adjust the pH to 6.0.

Biochar C700 and mineral fertiliser were integrated with various ratios to produce passivation agents, labelled as C10M0, C7M3, C5M5, C3M7, C0M10, and a control group. Six experimental groups were arranged in the leaching experiment utilising a column with a total height of 50 cm and an internal diameter of 4.5 cm. Each group was placed in a PVC pipe, cleaned, dried, and uniformly applied to the inner walls with petroleum jelly. The setup was successively filled from the bottom with a quartz sand layer of 1 cm thickness, a mixture of soil and passivation material (comprising 300 g of 10-mesh sieve-graded soil combined with 6 g of passivation materials), another quartz sand layer of 1 cm thickness, one

layer of nylon mesh, and one layer of plastic film. After completion, sufficient deionised water was added to achieve field capacity in the soil. The leaching apparatus is shown in Fig. 1. After allowing a week for soil ageing, on day 8, 100 mL of deionised water was added to moisturise the soil, initiating the leaching experiment on the day 9. Upon commencement, the leachate was introduced using a peristaltic pump, and it was collected every 24 hours for a period of 16 days. The collected samples were preserved at 4°C for analysis.

2.4. Analytical method

The sample was combined with deionised water at a ratio of 1∶2.5 solid-to-liquid, and the pH of the supernatant obtained post-centrifugation was assessed using a PHS-320 pH meter, which allowed for the determination of the pH of mineral fertilisers and soil specimens. The pH of biochar was gauged in a 1% (W/V) suspension in deionised water using an Orion pH meter (Thermo Electron Corp., USA). The Nitrogen Adsorption Multilayer Theory was utilised in conjunction with the ASAP-2020M analyser (Micromeritics Instrument Corp., USA) to measure the biochar's BET (Brunauer-Emmett-Teller) surface area. The concentration of heavy metals across all experiments was identified using the inductively coupled plasma mass spectrometer(ICP-MS, Thermo Fisher Scientific, USA). Rigorous quality control was maintained by the inclusion of blank and duplicate samples, ensuring the relative standard deviation (RSD) remained within the 5% range.

3. Results and discussion

3.1. Adsorption capacities of biochar and mineral fertilisers for cadmium and lead

3.1.1. Adsorption capacities for cadmium and lead in single solutions

The pyrolysis temperature of biochar significantly influences its properties. As summarized in Table 2 and Figure 2, the concentration, total adsorption, and removal rate of Cd and Pb in single solutions were compared after achieving adsorption equilibrium with different passivation agents. The adsorption efficiency of biochar pyrolyzed at different temperatures for Cd varies significantly: the higher the pyrolysis temperature, the greater the adsorption efficiency. For instance, the adsorption capacity of C700 reaches 4.21 mg/g, with an adsorption rate of 84.24%, whilst the least efficient C300 only has an adsorption capacity of 0.79 mg/g at an adsorption rate of 15.70%. This suggests that a higher pyrolysis temperature contributes to an improved adsorption effect of biochar for Cd. Unlike Cd, different passivation agents tend to have a higher adsorption quantity and rate for Pb in the solution, and the variance among them is relatively minimal, particularly with C600 and C700. Interestingly, the most efficient adsorbent for Cd, C700, only has a removal rate of 84.24%, which is 12.3% higher than the slightly less efficient C600. However, in the Pb adsorption experiment, C500 attained a removal rate of 89.16%, while C600 and C700 achieved significantly higher at 99.33% and 99.74%, respectively. Judging from the removal rate, biochar's adsorption performance for Pb surpasses that for Cd. Overall, mineral fertilizer performs best for Cd adsorption, while the adsorption efficiency for Pb slightly declines compared to C600 and C700, with C700 showing optimal adsorption capacity for Pb.

The principal mechanisms by which different types of biochar eliminate heavy metals include ion-exchange precipitation, functional group adsorption chelation, and cation-π interactions (Yang S et al., 2021). Pyrolysis

Table 2. Adsorption results of Cd and Pb in a single solution by biochar and mineral fertilizer.

Materials	Concentration/ (mg/L)		Adsorption capacity/ (mg/g)		Adsorption efficiency/%	
	Cd	Pb	Cd	Pb	Cd	Pb
C300	16.86	36.93	0.79	5.77	15.70%	38.44%
C400	14.95	13.37	1.26	11.66	25.25%	77.71%
C500	8.69	9.76	2.83	13.37	56.57%	89.16%
C600	5.61	0.40	3.60	14.90	71.94%	99.33%
C700	3.15	0.16	4.21	14.96	84.24%	99.74%
M	0.45	0.59	4.89	14.85	97.76%	99.01%

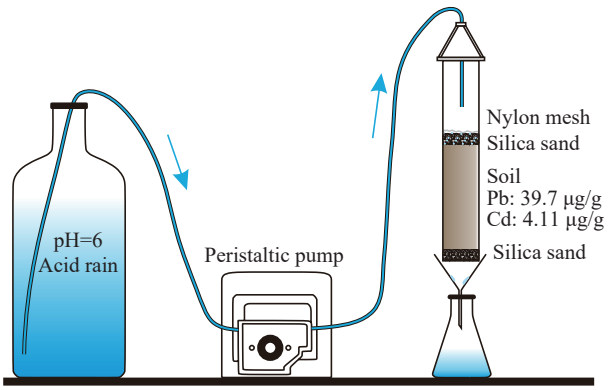

Fig. 1. Schematic diagram of leaching experiment (modified from Huang B et al., 2015).

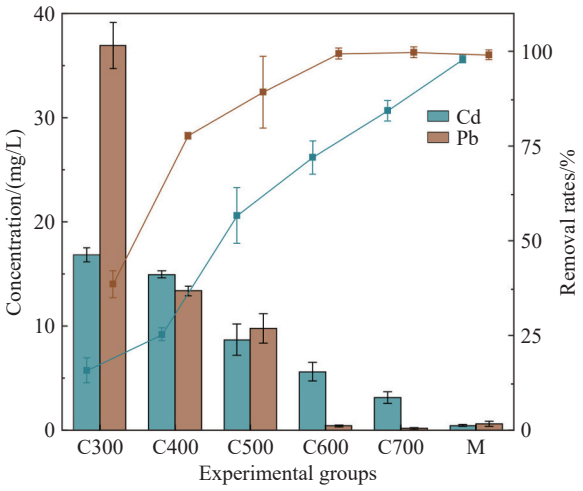

Fig. 2. Concentration and removal rate of Cd and Pb in a single-solution.

temperature influences the surface functional groups, density, porosity, and specific surface area, altering the adsorption capabilities of biochar (Yin D et al., 2017). This parameter is a crucial determinant in the capacity of biochar to adsorb heavy metals. Excessively high or low pyrolysis temperatures are detrimental to the adsorption capabilities of biochar (Li YC et al., 2020; Qiu BB et al., 2021). Within a certain range, higher pyrolysis temperatures result in the volatilization of organic acids and organic matter, thus increasing the biochar pH. This triggers the formation of additional ash residue and creates a more porous structure, thereby promoting ion adsorption (Ghysels S et al., 2019; Zheng LY and Wen JB, 2020; Cai RZ et al., 2022). As the temperature increases, the removal effectiveness of the prepared biochar incrementally improves. The optimal temperature for this process is approximately 700°C, as it yields the best removal results. However, exceeding this temperature results in a reduced removal rate (Zhang JZ et al., 2020; Fan FF and Zuo WY, 2022). This is attributed to excessively high pyrolysis temperatures that induce the expansion of pores, the merger of adjacent pores, or excessive ash residue, leading to pore obstruction and thereby causing a decrease in adsorption efficiency (Zong DP et al., 2023). Under the current experimental circumstances, the optimal biochar carbonization temperature is also 700°C. Biochar derived from rice husks that have been carbonized at this temperature exhibits a BET-specific surface area of 234.61 m^2/g and a pore volume of 0.16 cm^3/g, providing ample adsorption sites due to its increased surface area and pore volume (Tahir MH et al., 2019). Cation exchange, chelation, and precipitation are the primary mechanisms by which biochar adsorbs Cd and Pb (Li HB et al., 2017). Cation exchange is the dominant adsorption mechanism at higher pH, whereas the pyrolysis temperature influences the biochar's pH (Harvey OR et al., 2011). Functional group chelation is the secondary mechanism used by biochar to adsorb Cd and Pb. Hydroxyl groups can react with Cd (Ⅱ) to form Cd-O or Cd-OH compounds, while the cooperation of abundant functional groups, such as -OH- and -NH-, endows the biochar with commendable heavy metal ion adsorption performance (Xiang JX et al., 2021; Chen T et al., 2015; Yu WC et al., 2018). The alkaline elements within the biochar can also stimulate the acid functional groups to deprotonate, further enhancing adsorption capability. The substances within biochar, such as CO_3^{2-}, PO_4^{3-}, and OH^-, possess robust adsorption and binding capabilities with soil ions, which induce the conversion of free ions into a precipitate. (Hong MF et al., 2019; Rechberger MV et al., 2019; Cheng DL et al., 2020). Mineral fertilizers with high levels of Ca and Si, once applied, not only increase the pH of the solution and the negative charge of its surface but also promote the adsorption of heavy metal cations. After applying exogenous silicon in acidic soil, silicates adhere to the surface of the iron oxide in a polymer form, forming many negatively charged functional groups after silicate-iron chelation, providing more adsorption sites for Cd^{2+} and Pb^{2+} (Belton DJ et al., 2012). Additionally, the silicon ions released from soil silicates can combine with Cd^{2+} and Pb^{2+} to form silicon precipitate, diminishing its bioavailability (Xiao ZX et al., 2021).

3.1.2. Adsorption capacities for cadmium and lead in complex solutions.

The adsorption of heavy metals depends not only on the characteristics of the remedial agent but also on the nature of metal ions and their competitive behaviour for adsorption sites under complex conditions. Typically, the adsorption efficiency of competitive systems for heavy metal ions is lower than their single-ion adsorption behaviour (Park JH et al., 2016). As shown in Table 3 and Figure 3, the removal rate of Cd by biochar fluctuates significantly under complex conditions. The removal rates of Cd by C600 and C700 decrease by 68.29% and 63.79%, respectively. However, the removal rate of Pb changes minimally, indicating that Cd, which has a low affinity to biochar, is replaced by Pb, which has a high affinity. The removal rates of Cd and Pb by the mineral fertilizer only show a slight decrease.

Under identical experimental conditions, the distribution coefficient (K_d) is a valuable parameter for comparing the adsorption capabilities of different materials for any specific ion. Variations in the adsorption patterns of passivation agents can be confirmed by tracking changes in their distribution coefficient (Doumer ME et al., 2016). The higher distribution

Table 3. Adsorption results of Cd and Pb in a complex solution by biochar and mineral fertilizer.

Materials	Concentration (mg/L)		Adsorption capacity(mg/g)		Removal rate (compared to single solution, %)	
	Cd	Pb	Cd	Pb	Cd	Pb
C300	19.68	30.00	0.08	7.50	1.60(−14.10)	50.00(11.56)
C400	19.78	15.83	0.05	11.04	1.10(−24.15)	73.62(−4.09)
C500	19.55	5.86	0.11	13.54	2.25(−54.32)	90.23(1.08)
C600	19.27	0.95	0.18	14.76	3.65(−68.29)	98.42(−0.92)
C700	15.91	0.83	1.02	14.79	20.45(−63.79)	98.62(−1.12)
M	0.54	0.92	4.87	14.77	97.30(−0.46)	98.47(−0.54)

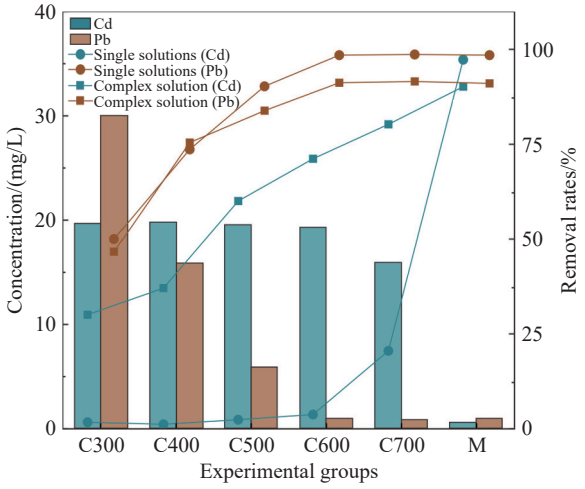

Fig. 3. Concentration and removal rate of Cd and Pb in a complex solution.

coefficient (K_d) indicates stronger adsorption and reduced solubility by the adsorbent. On the contrary, heavy metals with lower K_d can easily be replaced in competitive adsorption by heavy metals with higher K_d (Lee HS and Shin HS, 2021). The distribution coefficient (K_d) calculation methods are as follows (Khanverdiluo S et al., 2023).

$$\text{Distribution coefficients}(K_d) = \frac{\text{Equilibrium metal concentration adsorbed}}{\text{Equilibrium metal concentration in solution}} \quad (5)$$

In the formula, the equilibrium concentration of an adsorbed substance signifies the equilibrium metal content per unit weight of biochar and unit volume of the liquid solution.

The adsorption capacity of biochar and mineral fertilizers for all heavy metals is lower under mixed conditions than under single conditions, suggesting active competitive adsorption. As shown in Figure 4, Pb exhibits higher distribution coefficient (K_d), indicating that it is more likely to occupy adsorption sites than Cd, and this phenomenon is evident in all types of biochar. Under competitive conditions, the adsorption of heavy metal ions by passivation agents largely depends on the nature of the heavy metals, not the nature of the biochar (Lee HS and Shin HS, 2021). The smaller hydration radius of Pb^{2+} (4.01 Å) compared to Cd^{2+} (4.26 Å) determines Pb's greater adsorption affinity for most functional groups, including carboxyl and phenolic groups. Simultaneously, Pb (2.33) has a higher electronegativity than Cd (1.69), ensuring that Pb is easier to be adsorbed than Cd through inner-sphere complexation or adsorption reactions (Park JH et al., 2016). Overall, whether in the Cd-Pb complex solution or the single Pb or Cd solution, the mineral fertilizer outperforms rice husk biochar in its ability to adsorb Cd^{2+}, while C700 performs slightly better than the mineral fertilizer in adsorbing Pb^{2+}. This suggests that using biochar and mineral fertilizers in combination is crucial.

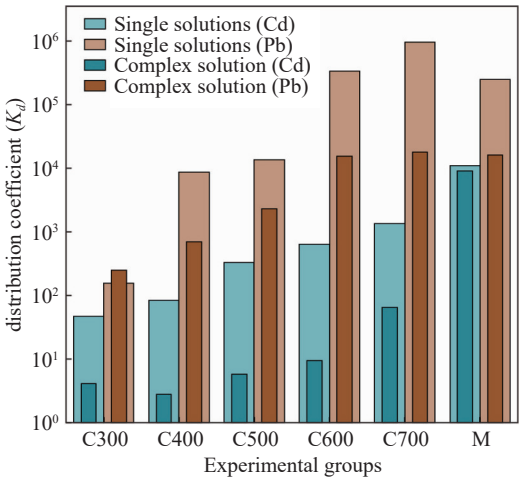

Fig. 4. Adsorption distribution coefficient (K_d) of Cd and Pb in single and complex solutions.

3.2. Isothermal adsorption models of different passivation agents for cadmium and lead

Isothermal adsorption curves describe the relationship between the concentration of the adsorbate at adsorption equilibrium and the amount of adsorbent adsorbed. They provide information about the adsorption process, such as the adsorption mechanism, maximum adsorption capacity, and characteristics of the adsorbent. This information plays a significant role in understanding the adsorption processes (Wang JL, Guo X, 2020; Yin ZB et al., 2020; Kalam S et al., 2021). During the adsorption experiment, whether under composite conditions or in single solutions of Pb^{2+} or Cd^{2+}, mineral fertilizer exhibited a markedly superior capacity for Cd adsorption compared to biochar. However, C700 was more effective in adsorbing Pb^{2+}. Based on these findings, isothermal adsorption experiments were conducted with C700 on Pb^{2+} and mineral fertilizer on Cd^{2+}. By changing the initial concentrations of Cd and Pb (5–320 mg/L), adsorption isotherms were established with a fixed dose of adsorbent to investigate the adsorption mechanism combined with existing experimental results. Fig. 5 and Table 4 show that the experimental results were fitted with the Langmuir and Freundlich isothermal adsorption equations. The deviation between the experimental and calculated data is represented by the correlation coefficient R^2. The isotherm equation with

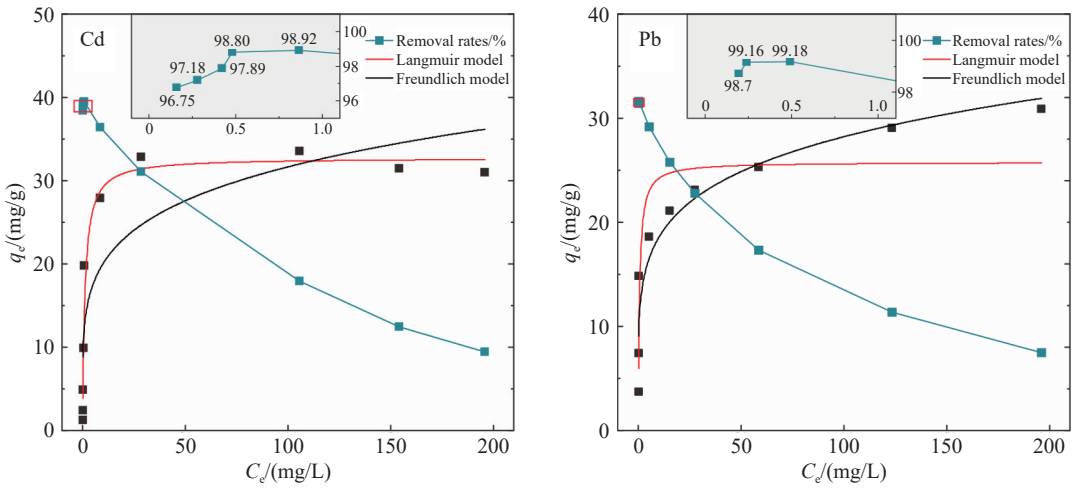

Fig. 5. Thermodynamic model for isothermal adsorption of Cd and Pb.

Table 4. Parameters of Cd and Pb isothermal adsorption models.

Samples	Langmuir model			Freundlich model			
	q_m (mg/g)	K_L (L/mg)	R^2	K_F[(mg$^{1-1/n}$·L$^{1/n}$)/g]	1/n	R^2	
Cd (M)	32.74	0.83	0.95	12.67	0.2	0.77	Present study
Pb (C700)	25.82	1.55	0.86	12.19	0.18	0.92	
Cd (C700)	6.72	0.069	0.793	−	0.219	0.524	(Dong YY et al., 2022)
Cd (M)	21.2	0.119	0.956	−	0.261	0.474	

the larger R^2 is closer to describing the adsorption process.

As illustrated in Fig. 5, with the increase in the initial solution concentration, the adsorption and removal rate of Cd^{2+} by mineral fertilizer continually rises, maintaining a high level. The onset of a certain concentration leads to slowed adsorption growth, eventually culminating in a peak value. As the initial concentration of Cd^{2+} continues to escalate, an eminent increase in adsorption follows until it reaches a certain concentration, when the adsorption increment decelerates or even demonstrates a slight dip. This trend is potentially determined by the amount of adsorbent added to the adsorption sites, which can be intensified by introducing passivation agents, thus enhancing the adsorption (Cai RZ et al., 2022). As the concentration of Cd^{2+} lies within 80 mg/L, the removal rate continuously experiences a mild incline, reaching its peak of 98.92% at the concentration of 80 mg/L. However, as the Cd^{2+} concentration soars to 120 mg/L, a persistent decrease in the removal rate occurs, ultimately plummeting to 38.78% at 320 mg/L. Similarly to mineral fertilizers, when the initial solution concentration is deficient, the adsorption of Pb^{2+} by C700 accelerates with increasing concentration while the momentum gradually decelerates yet persists in escalating. The removal rate of Pb^{2+} by C700 rises to 99.18% when the concentration of the Pb solution stands at 60 mg/L. As the Pb^{2+} concentration ascends to 80 mg/L, its removal rate witnesses a sustained ebb, eventually dropping to 38.66% at 320 mg/L. This peculiarity transpires because, when the Cd and Pb concentrations in the environment are low, ions can be swiftly absorbed onto the adsorbent sites; however, as the Cd and Pb concentrations intensify in the environment, a majority of the surface adsorption sites are swiftly occupied, leaving the residual Cd and Pb ions to diffuse into the inner pores of the adsorbent for adsorption. Consequently, reduced gradient and decelerated adsorption speed are observed, culminating in a balanced adsorption quantity.

The Langmuir model is the most frequent model utilized in gas-solid adsorption studies (Langmuir I, 1916, 1918), depicting an equilibrium scenario of monolayer uniform adsorption. In this scenario, the adsorbate distributes evenly across the adsorbent surface as a monolayer, culminating in the maximum adsorption capacity (Wang JL; Guo X, 2020). On the other hand, the Freundlich model is commonly employed to represent non-linear, multilayer adsorption phenomena (Freundlich H, 1907), delineating multilayer adsorption on heterogeneous surfaces (Wang CY et al., 2017; Zaheer Z et al., 2019), This means that it operates under the premise of a non-uniform adsorbent surface, simulating adsorbent behavior. After fitting the adsorption amount via the Langmuir and Freundlich models, the isotherm adsorption curve of Cd^{2+} by mineral fertilizer is more congruent with the Langmuir isotherm adsorption model. Consequently, for the adsorption of Cd by mineral fertilizer, homogeneous monolayer adsorption is more beneficial than non-uniform multilayer adsorption, and the adsorption of Cd^{2+} predominantly exists in monolayer adsorption (Chen ZM et al., 2012). The adsorption of Pb^{2+} by rice husk biochar is more compatible with the Freundlich model. Within the model's expression, the Langmuir constant K_L (L/mg), the ratio of adsorption and desorption rates exhibits the affinity between the adsorbent and the adsorbate. Both the theoretical adsorption capacity for Cd by mineral fertilizer and the K are significantly higher than those for Cd by C700, while the affinity for Pb by C700 (1.55) is remarkably more significant than that for Cd (0.069), aligning with experimental findings. An essential feature of the Langmuir constant R_L is its capacity to utilize the dimensionless constant of the separation factor to predict the affinity between the adsorbate and the adsorbent, determining whether a particular adsorption system is "favorable" or "unfavorable".

$$R_L = \frac{1}{1+K_L C_i} \tag{6}$$

K_L and C_i (mg/L) correspond to the Langmuir constant of the metallic ions utilized in this research and the initial ionic concentration. Typically, R_L<1 insinuates that the adsorption is favorable, R_L=0 denotes that the adsorption is irreversible, R_L=1 signifies a linear adsorption isotherm, and R_L>1 represents unfavorable adsorption (Barczak M et al., 2015;

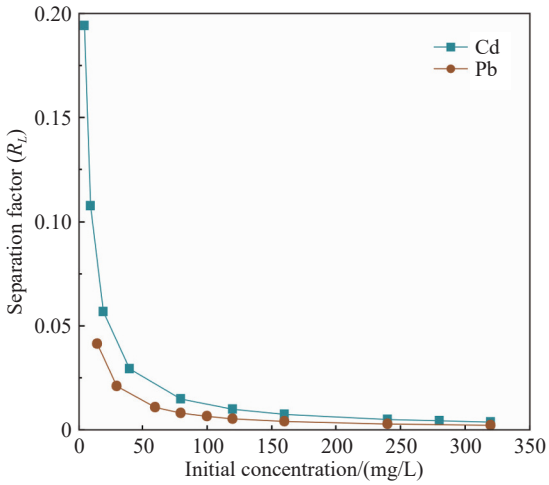

Fig. 6. Separation factor (R_L) for different initial concentrations.

Kalam S et al., 2021). As demonstrated in Figure 6, the increase in the initial concentrations of Cd and Pb leads to a decrease in R_L, signifying increased favorability towards ionic adsorption. However, as R_L approximates towards 0, it gradually becomes unfavorable for adsorption, aligning with findings where the removal rate declines as the concentration escalates.

Pertaining to the adsorption of Pb by biochar, the Freundlich fit results prove superior (R^2=0.92). K_F and n symbolize the adsorbent's capacity and the intensity (Wang TT et al., 2017). The larger the K_F, the stronger the adsorbent's adsorption capacity for heavy metal ions (Li JH et al., 2012). When 0<1/n<1, the adsorption is favorable; when 1/n>1, adsorption is unfavorable (Kalam S et al., 2021). In this study, all 1/n values are less than 1, indicating favorable adsorption processes. This signifies that the primary process for the adsorption of Pb by C700 involves non-linear adsorption, predominantly occurring on heterogeneous surfaces with multiple molecular layers, and exhibits a substantial adsorption capacity (Liu YD et al., 2011; Dai B et al., 2019).

3.3. Effect of different proportions of composite passivation agents on the leaching amount of Cd and Pb

Typically, the elution of ionic concentration diminishes with time progression (Van Poucke R et al., 2020). Following the addition of different passivation agents to the soil, changes in heavy metal leachate concentration are portrayed in Fig. 7, with the leachate solution concentrations of Cd and Pb decreasing as time transpires. Utilizing the fourth day as a pivot, within the 0–4 day period, Cd elution concentrations respectively dwindled by 53.29%–84.84%, while Pb's fell by 86.11%–93.66%. Pb's elution concentration plummets faster due to its superior occupancy of adsorption sites in a competing Cd, Pb adsorption system, preventing easy leaching with the solution. This is also evident in the initial concentrations of Cd and Pb in the leachate, where, although the soil Pb concentration (39.7 μg/g) exceeds that of Cd (4.11 μg/g), the Pb concentration in the leachate is lower.

The Cd and Pb leachate concentration variations across the six sample groups can generally be categorized into two. Firstly, the C10M0 (soil column supplemented solely with rice husk biochar) and the control group exhibit lower early-stage leachate concentrations that gradually increases, particularly for Pb, which, despite a brief dip, maintains a higher position from day two onwards. Secondly, the C7M3, C5M5, C3M7, and C0M10 groups display high initial concentrations that persistently and gradually decline.

When only the biochar is added to the soil, the introduction of biochar increases the soil pH and levels of organic matter, which later decrease over time. Experiments have indicated that the leachate concentration of heavy metal ions in soils treated with biochar increases over time but remains lower than control groups (O'Connor D et al., 2018). This resonates deeply with the observations from this experiment and can be attributed to changes in soil pH. Specifically, a decrease in soil pH over time leads to enhanced metal activity. Under simulated acid rain conditions, soil Pb is also mobilized, however, since the adsorption sites are occupied, it is not absorbed by the biochar, leading to a continuous increase in the leachate's Pb concentration (Fig. 7).

In the four experimental sets involving mineral fertilizers (C7M3, C5M5, C3M7, C0M10) the higher the proportion of mineral fertilizer, the greater the initial leaching concentration for Cd, and which decreased as the mineral fertilizer ratio was reduced. The group with the highest ratio, C0M10, attained a peak concentration 39.72 μg/L, 16.29 times greater than the biochar-only group and 3.89 times larger than that observed in the control group; Pb mirrors a similar concentration trend to Cd. Generally, biochar absorbs Cd^{2+} and Pb^{2+} at a faster pace, achieving equilibrium within several dozen minutes (Wang Q et al., 2017), while mineral fertilizer's adsorption of Cd^{2+} and Pb^{2+} is considerably slower, seemingly requiring several hours or even days for equilibrium. This is attributed to biochar's negatively charged surface quickly absorbing positively charged metal ions (Wang Q et al., 2017). In contrast, mineral fertilizers possess smaller specific surface areas and pore volumes, necessitating a dissolution and re-precipitation process before creating effective adsorption sites. In the later stages of leaching, the initially largest

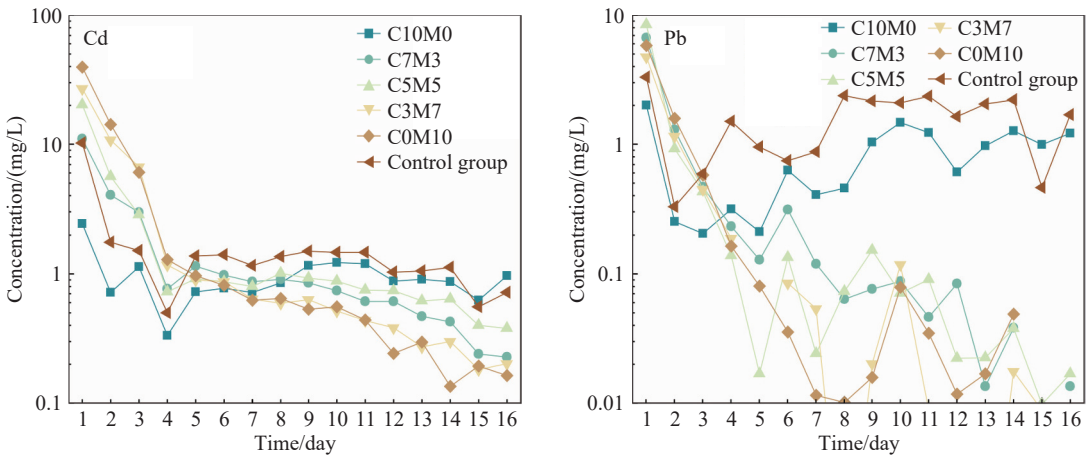

Fig. 7. Concentration of Cd and Pb in leachate.

concentration group, C0M10, gradually descends to the lowest, aligning with the known adsorption characteristics of biochar and mineral fertilizers. This highlights that the ratio of adsorbent is a critical influencer in the adsorption process (Chen T et al., 2015), and an increase in mineral fertilizer enhances adsorption stability (O'Connor D et al., 2018).

After adding amendments, the accumulated leaching concentrations still follow the rule of fast-then-slow in the leaching process (Fig. 8). The cumulative leaching amount of Cd under different amendment scenarios shows a similar temporal trend, characterized by two stages: Initial rapid leaching followed by a slower pace. Pb's cumulative leaching amounts are largely similar to Cd, with the exceptions being the C10M0 (soil column only supplemented with rice husk biochar) and the control group, both showing a continuous increase, directly corresponding with the daily concentration trends of Cd and Pb. Soil Cd predominantly exists in a weakly acidic extraction state and readily migrates back into the soil solution during weak acid leaching processes when external environments alter, and wherein mineral fertilizers cannot yet function fully, leading to a rapid increase in the initial leaching amount. Concurrently, due to Pb's competitive adsorption with Cd, the reduction speed in Cd's leaching concentration lags behind Pb.

Typically, the efficiency of composite amendments surpasses that of solitary ones. By coordinating the use of biochar and mineral fertilizer, the cumulative leaching of Cd and Pb can be significantly reduced. As demonstrated in Figure 9, the lowest total Pb leaching is observed in the C3M7 (a reduction of 74.62% compared to the control group) and C7M3 groups (a reduction of 72.91% compared to the control group). Conversely, Cd's total leaching quantity is majorly influenced by adding mineral fertilizer to the regenerative substance. The more mineral fertilizer added, the greater the total leaching volume of Cd. The minimum amount of Cd leaching is seen in the C10M0 (a reduction of 44.55% compared to the control group) and C7M3 groups (a reduction of 4.37% compared to the control group). To concurrently reduce the leaching of both Pb and Cd to a certain extent in leaching trials, the C7M3 formulation should be selected. Considering the natural degradation of biochar itself is incredibly slow (Zimmerman AR, 2010), biochar is often viewed as an inert substance within the timescale of most soil recovery projects, thus feasibly immobilizing soil pollutants for extended periods. During actual application, it is crucial to consider the ratio of different passivation agents in use.

4. Conclusions

In this study, adsorption experiments revealed that the higher the biochar pyrolysis temperature, the better the adsorption effect, with C700 proving to be the most effective biochar for adsorbing Cd^{2+} and Pb^{2+}. Also, C700 manifested a slightly better capacity for Pb^{2+} adsorption than mineral fertilizers, though its adsorption performance for Cd^{2+} was inferior. In the combined solution of Cd and Pb adsorption experiment, both biochar and mineral fertilizers exhibited less adsorption for Cd and Pb compared to solitary conditions, with Pb displaying a significantly higher distribution coefficient (K_d) than Cd, indicating vigorous competitive ion adsorption. The isothermal adsorption behaviour of mineral fertilizers for Cd obeys the Langmuir isothermal adsorption model, whereas C700's adsorption behaviour for Pb aligns more with the Freundlich isothermal adsorption model.

Combining mineral fertilizers and biochar outperforms single passivation agents in adsorbing heavy metals, effectively reducing the total amount of Cd and Pb leaching cumulatively in the soil. The two groups with the lowest total amount of Pb leaching are C3M7 and C7M3. In contrast, the least amount of Cd leaching is seen in C10M0 and C7M3. Considering these combined factors, the optimal formula to employ would be C7M3.

CRediT authorship contribution statement

Ze-ming Shi and Lü-han Yang conceived and planned the experiments. Lü-han Yang contributed to sample preparation and the interpretation of the results. Cheng-jie Zou wrote the manuscript with support from Na Zhang and Ying-hai Zhu. Ze-ming Shi supervised the project. All authors provided critical feedback and helped shape the research, analysis, and

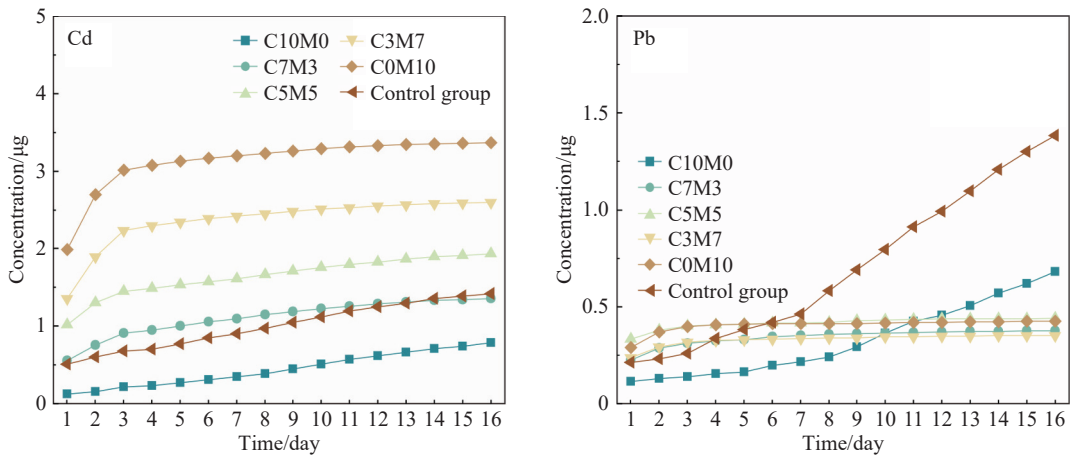

Fig. 8. Accumulated leaching amount of Cd and Pb in the leachate.

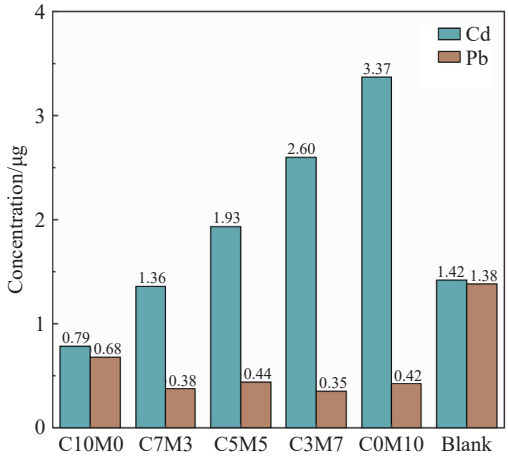

Fig. 9. Accumulated leaching amount of Cd and Pb in the different groups.

manuscript.

Declaration of competing interest

The authors declare no conflicts of interest.

Acknowledgment

This research was jointly supported by the National Natural Science Foundation of Sichuan Province (22NSFSC0191, 22NSFSC3990), and the research on key geological issues and uranium polymetallic ore target area in the Southwest China. Constructive comments by four anonymous reviewers have improved the manuscript.

References

Bao LR, Deng H, Jia ZM, Li Y, Dong JX, Yan MS, Zhang FL. 2020. Ecological and health risk assessment of heavy metals in farmland soil of Northwest Xiushan, Chongqing. Geology in China, 47(06), 1625–1636 (in Chinese with English abstract).

Barczak M, Michalak K, Gdula K, Tyszczuk K, Dobrowolski R, Dąbrowski A. 2015. Ordered mesoporous carbons as effective sorbents for removal of heavy metal ions. Microporous and Mesoporous Materials, 211, 162–173. doi: 10.1016/j.micromeso.2015.03.010.

Belton DJ, Deschaume O, Perry CC. 2012. An overview of the fundamentals of the chemistry of silica with relevance to biosilicification and technological advances. The FEBS Journal, 279(10), 1710–1720. doi: 10.1111/j.1742-4658.2012.08531.x.

Cai RZ, Tan CY, Cao XY, Ma YF, Liu LL, Cheng XY, Huang SP. 2022. Physico-chemical properties of pomelo peel biochar and its adsorption effect towards Cadmium. Journal Of Natural Science Of Hunan Normal University, 45(01), 57–66 (in Chinese with English abstract).

Chen T, Zhou ZY, Han R, Meng RH, Wang HT, Lu WJ. 2015. Adsorption of Cadmium by biochar derived from municipal sewage sludge: Impact factors and adsorption mechanism. Chemosphere, 134, 286–293. doi: 10.1016/j.chemosphere.2015.04.052.

Chen ZM, Fang Y, Xu YL, Chen BL. 2012. Adsorption of Pb^{2+} by rice straw derived-biochar and its influential factors. Acta Scientiae Circumstantiae, 32(04), 769–776 (in Chinese with English abstract). doi: 10.13671/j.hjkxxb.2012.04.018.

Cheng DL, Ngo HH, Guo WS, Chang SW, Nguyen DD, Zhang XB, Varjani S, Liu Y. 2020. Feasibility study on a new pomelo peel derived biochar for tetracycline antibiotics removal in swine wastewater. The Science of The Total Environment, 720, 137662. doi: 10.1016/j.scitotenv.2020.137662.

Dai B, Tan CY, Cao XY, Xie YC, Zhu SY, Bai J, Peng X. 2019. Physicochemical properties of biochar derived from lotus petiole and its adsorption mechanism of Cadmium in aqueous solution. Research Of Environmental Sciences, 32(03), 513–522 (in Chinese with English abstract). doi: 10.13198/j.issn.1001-6929.2018.11.27.

Dong YY, Shi ZM, Wang XY, Yang LH, Zhang JJ. 2022. Characteristics of Cadmium adsorption and soil cadmium passivation by biochar mixed with mineral fertilizer. Guangzhou Chemical Industry, 50(05), 36–39 (in Chinese with English abstract).

Doumer ME, Rigol A, Vidal M, Mangrich AS. 2016. Removal of Cd, Cu, Pb, and Zn from aqueous solutions by biochars. Environmental Science and Pollution Research, 23(3), 2684–2692. doi: 10.1007/s11356-015-5486-3.

Fan FF, Zuo WY. 2022. Effect of preparation conditions on the adsorption capacity of methylene blue by rice husk biochar. Anhui Chemical Industry, 48(06), 66–69 (in Chinese with English abstract).

Freundlich H. 1907. Über die adsorption in Lösungen. Zeitschrift für Physikalische Chemie, 57U(1), 385–470. doi: 10.1515/zpch-1907-5723.

Ghysels S, Ronsse F, Dickinson D, Prins W. 2019. Production and characterization of slow pyrolysis biochar from lignin-rich digested stillage from lignocellulosic ethanol production. Biomass and Bioenergy, 122, 349–360. doi: 10.1016/j.biombioe.2019.01.040.

Harvey OR, Herbert BE, Rhue RD, Kuo LJ. 2011. Metal interactions at the biochar-water interface: energetics and structure-sorption relationships elucidated by flow adsorption microcalorimetry. Environmental Science and Technology, 45(13), 5550–5556. doi: 10.1021/es104401h.

He YB, Huang D, Zhu Q, Wang S, Liu SL, He HB, Zhu HH, Xu C. 2017. A three-season field study on the in-situ remediation of Cd-contaminated paddy soil using lime, two industrial by-products, and a low-Cd-accumulation rice cultivar. Ecotoxicology and Environmental Safety, 136, 135–141. doi: 10.1016/j.ecoenv.2016.11.005.

Hong MF, Zhang LM, Tan ZX, Huang QY. 2019. Effect mechanism of biochar's zeta potential on farmland soil's cadmium immobilization. Environmental Science and Pollution Research, 26(19), 19738–19748. doi: 10.1007/s11356-019-05298-5.

Huang B, Li ZW, Huang JQ, Chen GQ, Nie XD, Ma WM, Yao HB, Zhen JM, Zeng GM. 2015. Aging effect on the leaching behavior of heavy metals (Cu, Zn, and Cd) in red paddy soil. Environmental Science and Pollution Research, 22(15), 11467–11477. doi: 10.1007/s11356-015-4386-x.

Kalam S, Abu-Khamsin SA, Kamal MS, Patil S. 2021. Surfactant adsorption isotherms: A review. ACS Omega, 6(48), 32342–32348. doi: 10.1021/acsomega.1c04661.

Khanverdiluo S, Talebi, Ghane, Elaheh, Ranjbar A, Mehri F. 2023. Content of potentially toxic elements (PTEs) in various animal meats: a meta-analysis study, systematic review, and health risk assessment. Environmental Science and Pollution Research, 30(6), 14050–14061. doi: 10.1007/s11356-022-24836-2.

Langmuir I. 1916. The constitution and fundamental properties of solids and liquids. Part Ⅰ. solids. Journal of The American Chemical Society, 38(11), 2221–2295. doi: 10.1021/ja02268a002.

Langmuir I. 1918. The adsorption of gases on plane surfaces of glass, mica and platinum. Journal of The American Chemical Society, 40(9), 1361–1403. doi: 10.1021/ja02242a004.

Lee HS, Shin HS. 2021. Competitive adsorption of heavy metals onto modified biochars: Comparison of biochar properties and modification methods. Journal of Environmental Management, 299,

113651. doi: 10.1016/j.jenvman.2021.113651.

Li HB, Dong XL, Da Silva EB, Oliveira LM de, Chen YS, Ma LQ. 2017. Mechanisms of metal sorption by biochars: Biochar characteristics and modifications. Chemosphere, 178, 466–478. doi: 10.1016/j.chemosphere.2017.03.072.

Li JH, Lv GH, Bai WB, Guo JY, Song JQ, Zhang QZ. 2012. Effect of modified biochar on soil nitrate nitrogen and available phosphorus leaching. Chinese Journal Of Agrometeorology, 33(02), 220–225 (in Chinese with English abstract).

Li YC, Xing B, Ding Y, Han XH, Wang SR. 2020. A critical review of the production and advanced utilization of biochar via selective pyrolysis of lignocellulosic biomass. Bioresource Technology, 312, 123614. doi: 10.1016/j.biortech.2020.123614.

Liang LP, Xi FF, Tan WS, Meng X, Hu BW, Wang XK. 2021. Review of organic and inorganic pollutants removal by biochar and biochar-based composites. Biochar, 3(3), 255–281. doi: 10.1007/s42773-021-00101-6.

Lin J, Liang WJ, Jiao Y, Yang L, Fan YN, Tian T, Liu XM. 2021. Ecological and health risk assessment of heavy metals in farmland soil around the gold mining area in Tongguan of Shaanxi Province. Geology In China, 48(03), 749–763 (in Chinese with English abstract).

Liu RP, Xu YN, Zhang JH, Wang WK, Elwardany RM. 2020. Effects of heavy metal pollution on farmland soils and crops: A case study of the Xiaoqinling Gold Belt, China. China Geology, 3(3), 402–410. doi: 10.31035/cg2020024.

Liu YD, Chae HG, Kumar S. 2011. Gel-spun carbon nanotubes/polyacrylonitrile composite fibers. Part II: Stabilization reaction kinetics and effect of gas environment. Carbon, 49(13), 4477–4486. doi: 10.1016/j.carbon.2011.06.042.

Lv XY, Shi ZM, Zhang JJ, Hou Y, Huang WW. 2022. Study on leaching characteristics of Cadmium from soil by composite mineral materials. Computing Techniques For Geophysical and Geochemical Exploration, 44(03), 366–374 (in Chinese with English abstract).

O'Connor D, Peng T, Zhang J, Tsang DCW, Alessi DS, Shen Z, Bolan NS, Hou D. 2018. Biochar application for the remediation of heavy metal polluted land: A review of in situ field trials. The Science of The Total Environment, 619-620, 815–826. doi: 10.1016/j.scitotenv.2017.11.132.

Osman AI, Fawzy S, Farghali M, El-Azazy M, Elgarahy AM, Fahim RA, Maksoud AM, Ajlan AA, Yousry M, Saleem Y, Rooney DW. 2022. Biochar for agronomy, animal farming, anaerobic digestion, composting, water treatment, soil remediation, construction, energy storage, and carbon sequestration: A review. Environmental Chemistry Letters, 20(4), 2385–2485. doi: 10.1007/s10311-022-01424-x.

Park JH, Ok YS, Kim SH, Cho JS, Heo JS, Delaune RD, Seo DC. 2016. Competitive adsorption of heavy metals onto sesame straw biochar in aqueous solutions. Chemosphere, 142, 77–83. doi: 10.1016/j.chemosphere.2015.05.093.

Qiu BB, Tao XD, Wang H, Li WK, Ding X, Chu HQ. 2021. Biochar as a low-cost adsorbent for aqueous heavy metal removal: A review. Journal Of Analytical and Applied Pyrolysis, 155, 105081. doi: 10.1016/j.jaap.2021.105081.

Rechberger MV, Kloss S, Wang SL, Lehmann J, Rennhofer H, Ottner F, Wriessnig K, Daudin G, Lichtenegger H, Soja G, Zehetner F. 2019. Enhanced Cu and Cd sorption after soil aging of woodchip-derived biochar: What were the driving factors? Chemosphere, 216: 463–471. doi: 10.1016/j.chemosphere.2018.10.094.

Rushimisha IE, Li XJ, Han T, Chen XD, Abdoul MASI, Sun Y, Li YT. 2022. Application of biochar on soil bioelectrochemical remediation: behind roles, progress, and potential. Critical Reviews In Biotechnology: 1–19. doi: 10.1080/07388551.2022.2119547.

Shi Z M. 2014. Study on source identification and risk assessment methods of heavy metal elements such as Cadmium in surface soil of southwest China[R]. Chengdu, Geological Survey Institute of CDUT.

Tahir MH, Çakman G, Goldfarb JL, Topcu Y, Naqvi SR, Ceylan S. 2019. Demonstrating the suitability of canola residue biomass to biofuel conversion via pyrolysis through reaction kinetics, thermodynamics and evolved gas analyses. Bioresource Technology, 279, 67–73. doi: 10.1016/j.biortech.2019.01.106.

Van Poucke R, Meers E, Tack FMG. 2020. Leaching behavior of Cd, Zn and nutrients (K, P, S) from a contaminated soil as affected by amendment with biochar. Chemosphere, 245, 125561. doi: 10.1016/j.chemosphere.2019.125561.

Wang CY, Boithias L, Ning ZG, Han YP, Sauvage S, Sánchez Pérez JM, Kuramochi K, Hatano R. 2017. Comparison of Langmuir and Freundlich adsorption equations within the SWAT-K model for assessing potassium environmental losses at basin scale. Agricultural Water Management, 180, 205–211. doi: 10.1016/j.agwat.2016.08.001.

Wang JL, Guo X. 2020. Adsorption isotherm models: Classification, physical meaning, application and solving method. Chemosphere, 258, 127279. doi: 10.1016/j.chemosphere.2020.127279.

Wang P, Chen HP, Kopittke PM, Zhao FJ. 2019. Cadmium contamination in agricultural soils of China and the impact on food safety. Environmental Pollution (Barking, Essex : 1987), 249: 1038–1048. doi: 10.1016/j.envpol.2019.03.063.

Wang Q, Wang BW, Tan GC, Xu N. 2017. Single and competitive adsorption of Cu (Ⅱ), Pb (Ⅱ), Ni (Ⅱ) and Cd (Ⅱ) onto biochar. Acta Scientiarum Naturalium Universitatis Pekinensis, 53(06), 1122–1132 (in Chinese with English abstract). doi: 10.13209/j.0479-8023.2017.130.

Wang TT, Ma JB, Qu D, Zhang XY, Zheng JY, Zhang XC. 2017. Characteristics and mechanism of Copper adsorption from aqueous solutions on biochar produced from sawdust and apple branch. Environmental Science, 38(05), 2161–2171 (in Chinese with English abstract). doi: 10.13227/j.hjkx.201610124.

Xiang JX, Lin Q, Yao XS, Yin GC. 2021. Removal of Cd from aqueous solution by chitosan coated MgO-biochar and its in-situ remediation of Cd-contaminated soil. Environmental Research, 195, 110650. doi: 10.1016/j.envres.2020.110650.

Xiao ZX, Peng M, Mei YC, Tan L, Liang YC. 2021. Effect of organosilicone and mineral silicon fertilizers on chemical forms of cadmium and lead in soil and their accumulation in rice. Environmental Pollution (Barking, Essex: 1987), 283: 117107. doi: 10.1016/j.envpol.2021.117107.

Xu HL, Li MR, Jiang H, Yang QF, Zhao JW, Hu SX, Zhou XJ. 2021. Ecological geochemical risk assessment of cadmium in soil-sediment of Danjiangkou Reservoir. Geology In China, 48(04), 1166–1176 (in Chinese with English abstract).

Xu Y, Liang XF, Xu YM, QIN X, HUANG QQ, Wang L, Sun YB. 2017. Remediation of heavy metal-polluted agricultural soils using clay minerals: A Review. Pedosphere, 27(2), 193–204. doi: 10.1016/S1002-0160(17)60310-2.

Yang L, Zhang Z, Li YJ, Wang C, Weng ZF, Zhang ZY. 2018. Adsorption characteristics of Cd^{2+} and Pb^{2+} in typical agricultural soils in the Southwest of China. Chinese Journal Of Soil Science, 49(04), 985–992 (in Chinese with English abstract). doi: 10.19336/j.cnki.trtb.2018.04.33.

Yang S, Wen QX, Chen ZQ. 2021. Effect of KH_2PO_4-modified biochar on immobilization of Cr, Cu, Pb, Zn and as during anaerobic digestion of swine manure. Bioresource Technology, 339, 125570. doi: 10.1016/j.biortech.2021.125570.

Yin D, Wang X, Peng B, Tan C, Ma LQ. 2017. Effect of biochar and Fe-biochar on Cd and As mobility and transfer in soil-rice system. Chemosphere, 186, 928–937. doi: 10.1016/j.chemosphere.2017.

07.126.

Yin ZB, Xu S, Liu S, Xu SY, Li JH, Zhang YC. 2020. A novel magnetic biochar prepared by K2FeO4-promoted oxidative pyrolysis of pomelo peel for adsorption of hexavalent chromium. Bioresource Technology, 300, 122680. doi: 10.1016/j.biortech.2019.122680.

Yu WC, Lian F, Cui GN, Liu ZQ. 2018. N-doping effectively enhances the adsorption capacity of biochar for heavy metal ions from aqueous solution. Chemosphere, 193, 8–16. doi: 10.1016/j.chemosphere.2017.10.134.

Zaheer Z, AL-Asfar A, Aazam ES. 2019. Adsorption of methyl red on biogenic Ag@Fe nanocomposite adsorbent: Isotherms, kinetics and mechanisms. Journal Of Molecular Liquids, 283, 287–298. doi: 10.1016/j.molliq.2019.03.030.

Zhang JZ, Hou DY, Shen ZT, Jin F, O'Connor D, Pan SZ, Ok YS, Tsang DC, Bolan NS, Alessi DS. 2020. Effects of excessive impregnation, magnesium content, and pyrolysis temperature on MgO-coated watermelon rind biochar and its lead removal capacity. Environmental Research, 183, 109152. doi: 10.1016/j.envres.2020.109152.

Zhang JJ. 2021. Restoration Mechanism of Soils Contaminated with Cadmium and Lead by A Novel Composite Mineral Remediation Agent. Chengdu, Chengdu University of Technology, Ph. D thesis, 1–115 (in Chinese with English abstract).

Zhang K, Yi YQ, Fang ZQ. 2023. Remediation of cadmium or arsenic contaminated water and soil by modified biochar: A review. Chemosphere, 311, 136914. doi: 10.1016/j.chemosphere.2022.136914.

Zheng LY, Wen JB. 2020. Effect of pyrolysis temperature on heavy metal contaminated soil passed by straw biochar. Science Technology and Engineering, 20(16), 6683–6687 (in Chinese with English abstract).

Zimmerman AR. 2010. Abiotic and microbial oxidation of laboratory-produced black carbon (biochar). Environmental Science and Technology, 44(4), 1295–1301. doi: 10.1021/es903140c.

Zong DP, Tian W, Li WY, Zhang MY, Xu WM. 2023. Mechanisms of heavy metals passivation in soils by biochar derived from agricultural and forestry wastes: A Review. Asian Journal Of Ecotoxicology, 18(1), 232–245 (in Chinese with English abstract).